Picosecond measurements of relaxation of internal modes in crystalline benzene as a function of temperature

Renato Torre, Roberto Righini, Leonardo Angeloni, and Salvatore Califano
Dipartimento di Chimica, Università di Firenze, Via Gino Capponi 9, 50121 Florence, Italy
European Laboratory of Nonlinear Spectroscopy, Largo Enrico Fermi, 2-50125 Florence, Italy

(Received 9 February 1990; accepted 17 April 1990)

The relaxation rates of four internal vibrational levels of benzene crystal have been measured by time-resolved coherent anti-Stokes Raman scattering (CARS) at different temperatures. The important information on the dephasing mechanisms provided by the experiment has been supported by anharmonic calculations, which include the full contribution of the density of phonon states, by utilizing average coupling coefficients. Different behaviors have been observed for the different modes considered. Three of the four vibrations (v_1,v_6, and v_{10}) show linewidths that increase linearly in the classical regime with temperature; the experimental evidence for the important role played by three-phonon processes (driven by cubic anharmonicity) is confirmed by the calculations, which give a quantitative agreement with the observed linewidths. For the above-mentioned vibrations the role of pure dephasing results in a minor contribution, while the effect of isotopic impurities is important in determining the low temperature relaxation rate. On the other hand, the linewidth of v_9 increases quadratically with T: Both decay processes of high order and pure dephasing may be responsible for such a behavior. This ambiguity cannot be overcome by our calculations, since these do not include the effect of high order (mainly quartic) anharmonic terms. Finally, the analysis of the decay mechanisms as predicted by the calculation shows that the anharmonic coefficients may differ from mode to mode: the relaxation mechanism is highly mode selective, and its efficiency depends greatly on the nature of the molecular normal coordinates involved in the process.

I. INTRODUCTION

The interpretation of the mechanisms of vibrational relaxation in molecular solids is often much simpler than in other condensed phases. Calculations based on the perturbative approach[1] have been shown to be of great value in elucidating the possible relaxation routes in different crystals; in this way, although the amount of experimental data available on this subject is still limited, a relatively clear picture of the main processes involved in the relaxation of phonon states has been achieved.

There are some peculiar aspects of vibrational relaxation in crystals that deserve special consideration:

(i) Inhomogenous broadening of the spectral lines is practically absent in perfect crystals; in real crystals the inhomogenous contribution to the line shape is averaged out, due to motional narrowing.

(ii) The pattern of vibrational levels is substantially modified in solids with respect to the isolated molecule by the quasicontinuum of low-frequency (<200 cm -1) lattice vibrations and by the dispersion of the internal modes. Such a difference has great influence on the relaxation mechanisms.

(iii) The zero-order states are exactly described in the harmonic approximation in terms of delocalized crystal states, including those of the thermal bath. The vibrational relaxation can be taken into account by including anharmonic terms which mix the zero-order states; many-body perturbative techniques provide the basis for such a description, with no need for ensemble statistical average.

From the spectroscopic point of view, vibrational relaxation results in a dephasing of the excitation which, in the absence of inhomogeneous effects, determines the linewidths of the transition. Alternatively, the same effect can be observed in phase-sensitive time-resolved experiments, in which the coherence lifetime T_2 is measured. The half-band width Γ and the dephasing time are related by

$$2\Gamma = (\pi c T_2)^{-1}.$$

The experimental linewidth (or the inverse dephasing time) contains the contributions of population decay processes and of pure dephasing.

Population decay is a process in which energy is transferred from the excited states to other states of the system via anharmonic interactions.[1,2] Since energy and momentum must be conserved in the process, the pattern of the density of phonon states of the crystal plays a crucial role. The lifetime related to energy decay is indicated by T_1.

No energy exchange is instead implied in pure dephasing, characterized by a T_2^* time: the role of the anharmonic interactions is that of modulating the phonon energies, without modifying the population distribution.[1-4] The observed total dephasing time T_2 is the result of both kinds of processes, according to

$$1/T_2 = 1/2T_1 + 1/T_2^*.$$

In molecular solids the lattice vibrations, extending from $\omega > 0$ to a few hundreds of wave numbers, may easily provide the phonon states of the appropriate frequency for energy-conserving transfer of the excitation to a different phonon level. As a result, population decay in molecular crystals is expected to be more important than, for instance,

 0021-9606/90/172967-07$03.00

in liquids, becoming at least competitive with pure dephasing processes.

Internal vibrations of molecular crystals are, in this respect, a special case; in fact, they are, at least in simple molecules, rather isolated, so that the number of possible decay channels is generally small. The interpretation in terms of decay mechanisms is then made simpler.

We recently reported on the vibrational relaxation of internal modes in a number of molecular-ionic crystals (K_2SO_4,[5] $CaCO_3$,[6] $KClO_4$,[7] $NaNO_3$,[8]) and in simple molecular crystals (CO_2,[9] SO_2[10]). The results obtained for the different systems show that the temperature dependence of the relaxation times (or, equivalently, of the linewidths) provides fundamental information on the prevailing mechanisms leading to vibrational relaxation. Here we extend such analysis to four internal vibrations of crystalline benzene in a wide temperature range (10–200 K).

The many-body perturbative treatment of vibrational relaxation in molecular crystals has been widely discussed in a number of papers and books; the specific case of molecular crystals is covered in the book by Califano *et al.*[2] Here we recall only few fundamental aspects which are relevant to the subsequent discussion.

The phonon–phonon interactions leading to energy relaxation are separated into contributions of different order in the perturbative expansion. The members of the series are generally represented by diagrams, in which the lines represent harmonic phonon propagators and the vertices are the anharmonic coupling coefficients. For instance, the diagrams

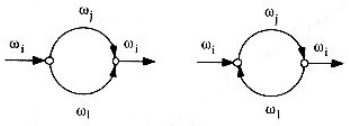

three phonon down conversion process — three phonon up conversion process

represent three-phonon scattering processes, whose contribution to the linewidth 2Γ of the $\omega_i(0)$ phonon is given by

$$\Gamma\omega_i(0) = 18\pi\hbar^2 \sum_k \sum_{jl} \left| B \begin{pmatrix} i & j & l \\ 0 & k & -k \end{pmatrix} \right|^2 \times \{(n_{jk} + n_{lk} + 1)\delta(\omega_i(0) - \omega_j(k) - \omega_l(k)) + 2(n_{jk} - n_{lk})\delta(\omega_i(0) + \omega_j(k) - \omega_l(k))\}. \quad (1)$$

In the previous expression n_{jk} is the thermally averaged occupation number of the phonon $\omega_j(k)$:

$$n_{jk} = [\exp(h\omega_j(k)/K_B T) - 1]^{-1}.$$

B is the coupling coefficient depending on the cubic anharmonicity, and $\delta(\omega)$ is a Dirac delta function which accounts for the possible decay channels in the two-phonon density of states. The first term in the right-hand side of Eq. (1) describes a down-conversion process, while the second term represents an up-conversion process, which requires thermal population of the $\omega_j(k)$ phonons.

As pointed out in previous papers, the temperature dependence of the linewidth provides the clue to discriminate between the possible different terms contributing to the overall relaxation. In fact, expression (1) predicts a linear dependence of the width 2Γ on the occupation numbers; higher-order perturbation terms (involving four-phonon processes, or multiple three-phonon scattering) are described by more complex diagrams, whose expressions contain products of occupation numbers.[1] Since for $h\omega < K_B T$ the occupation number is proportional to T, a linear dependence of 2Γ on the temperature is expected in the classical regime for relaxation processes dominated by mechanisms of type (1), while a quadratic or a higher-order behavior is predicted when higher-order processes become important.

At the moment, the only experimental data on aromatic crystals covering a wide temperture range are those concerning the lattice vibrations of naphthalene[11–13] and anthracene[13,14] crystals. Liquid He temperature values are available for the linewidths (or lifetimes) of some internal modes of benzene,[15–17] while data at different temperatures have been published for some internal vibrations of naphthalene[13,18–23] and anthracene.[13] The relaxation time for the 766 cm^{-1} ν_8 mode of naphthalene has also been calculated by Righini[24] in the temperature range 4–150 K.

In the present paper we present the results obtained by means of time-resolved coherent anti-stokes Raman scattering (CARS) spectroscopy for the totally symmetric factor group components of four internal modes of benzene crystal between 10 and 200 K. The experiments were limited to the low-frequency part ($< 1200\ cm^{-1}$) of the Raman spectrum (ν_6, ν_{10}, ν_1, and ν_9) in view of the congestion of the spectral region at higher frequencies.

II. EXPERIMENTAL

Spectrophotometric grade benzene was first purified by repeated treatment with concentrated sulfuric acid, and then distilled. The crystals used in the experiments were grown in a quartz cell (10×20 mm, 1 mm thick). The cell was sealed in vacuum and closed in a copper holder, the thermal contact being ensured by an indium gasket. The copper holder was placed on the cold tip of a closed circuit He cryostat, equipped with a silicon diode temperature detector. The sample temperature was controlled by means of a resistor driven by a computerized temperature controller.

Very good quality single crystals were grown by very slow cooling of the sample (0.2 K/h). Depending on the shape of the indium gasket between the quartz cell and the copper holder, different temperature gradients set up inside the cell, resulting in different orientation of the single crystal. After several attempts, we were able to obtain samples with one crystal axis parallel to the long dimension of the cell. The polarization discrimination between the different factor group splitting components was thus possible with appropriate CARS geometry.

The CARS setup has been described in previous papers;[5,7] in short, a mode-locked Ar^+ laser is used to synchronously pump two dye lasers, delivering pulses about 5 ps long and at frequencies ω_1 and ω_2. The higher frequency beam ω_1 is split in two: one part is used with ω_2 to excite the Raman transition, while the second part is used as a probe beam, after passing through a variable delay line. The inten-

sity of the antistokes beam is measured by a photon-counting system coupled to a double monochromator. Over six decades of CARS signal can be measured in the most favorable cases.

For very weak signals, when the resonant part of comparable or smaller than the nonresonant contribution and for short decay times, an accurate determination of the signal decay time requires a deconvolution procedure. The deconvolution technique adopted in the present work takes into account the temporal shape of the laser pulses and the contribution of the nonresonant background. The overall signal is obtained as the sum of different contributions

$$S(t) = |P_1|^2 + |P_2|^2 + 2P_1P_2 + |P_{\mathrm{NR}}|^2 + 2P_{1\mathrm{NR}} + 2P_{2\mathrm{NR}},$$

where

$$|P_1|^2 = \int_{-\infty}^{\infty} dt \left\{ |E_1(t-\tau)|^2 \int_{-\infty}^{t} dt' E_1(t') E_2^*(t') R(t'-t) \times \int_{-\infty}^{t} dt'' E_1^*(t'') E_2(t'') R^*(t''-t) \right\},$$

$$|P_2|^2 = \int_{-\infty}^{\infty} dt \left\{ |E_1(t)|^2 \int_{-\infty}^{t} dt' E_2^*(t') E_1(t'-\tau) R(t'-t) \times \int_{-\infty}^{t} dt'' E_1(t''-\tau) E_2^*(t'') R^*(t''-t) \right\},$$

$$P_1P_2 = \mathrm{Re}\left\{ \int_{-\infty}^{\infty} dt \left[E_1(t-\tau) E_1^*(t) \times \int_{-\infty}^{t} dt' E_1(t') E_2^*(t') R(t'-t) \times \int_{-\infty}^{t} dt'' E_1^*(t'') E_2(t'') R^*(t''-t) \right] \right\}$$

$$|P_{\mathrm{NR}}|^2 = \int_{-\infty}^{\infty} dt \{ |\chi_{\mathrm{NR}}|^2 |E_1(t)|^2 E_2(t)|^2 |E_1(t-\tau)|^2 \},$$

$$P_{1\mathrm{NR}} + P_{2\mathrm{NR}} = \mathrm{Re}\,\chi_{\mathrm{NR}} \int_{-\infty}^{\infty} dt \left\{ |E_1(t-\tau)|^2 E_1^*(t) E_2(t) \times \int_{-\infty}^{t} dt' E_2^*(t') E_1(t') R(t'-t) + |E_1(t)|^2 E_1^*(t-\tau) E_2(t) \times \int_{-\infty}^{t} dt' E_2^*(t') E_1(t'-\tau) R(t'-t) \right\}.$$

$|P_1|^2$ and $|P_2|^2$ describe the contributions to the signal when the role of probe beam is interchanged between ω_1 and ω_1'; P_1P_2 is the cross term of the two; $|P_{\mathrm{NR}}|^2$ is the contribution from the nonresonant background; $P_{1\mathrm{NR}}$ and $P_{2\mathrm{NR}}$ are the cross terms between the resonant and the nonresonant contributions; they vanish when the response function $R(t)$ is real, i.e., when the detuning is zero.

$E_1(t)$ and $E_2(t)$ represent the temporal profile of the laser pulses in the ω_1 and ω_2 beams, respectively: a biexponential function was adopted in both cases. $R(t)$ is the response function of the system and includes the exponential decay due to the vibrational dephasing. The $|\chi_{\mathrm{NR}}|^2$ parameter gives the nonresonant contribution as a fraction of the resonant signal. Details on the derivation of the equations given above for the deconvolution procedure will be given in a forthcoming paper.[25]

The quality of the fit obtained is shown in Fig. 1. A biexponential function of the type

$$E(t) = \begin{cases} E\exp(\delta\gamma t) & \text{for } t<0 \\ E\exp(-\gamma t) & \text{for } t>0 \end{cases}$$

was used. The δ and γ parameters were obtained from the experimental auto- and cross-correlation traces of the pulse intensity. The final FWHM values resulted 6 ps for ω_1 and ω_2 with $\delta = 1.3$.

III. RESULTS AND DISCUSSION

As already mentioned in Sec. I, time-resolved CARS, as a technique based on a coherent effect, is intrinsically unable to discriminate between the different contributions to vibrational relaxation. However, the temperature dependence of the measured CARS signal decay time represents a fundamental contribution to elucidate some aspects of the problem which are still open to investigation: (i) the relative importance of energy decay T_1 and pure dephasing T_2^*; (ii) the relative weights of the different multiphonon scattering processes responsible for the T_1 relaxation rate; (iii) the role of crystal defects and impurities.

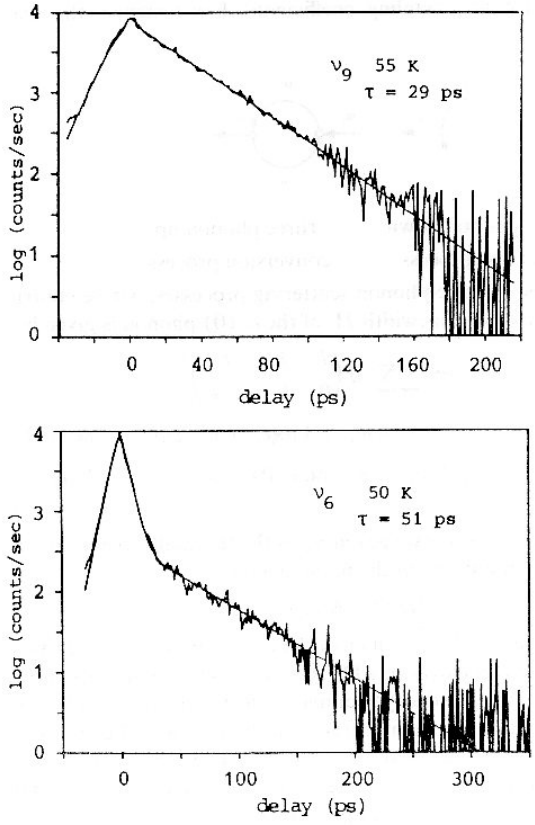

FIG. 1. CARS signal decay profiles measured for ν_9 and ν_6. The fit was obtained by means of the deconvolution procedure given in the text.

TABLE I. Low temperature CARS signal decay times and bandwidths of crystalline benzene.

			Our results		Ref. 17
Mode	ν (cm^{-1})	T (K)	τ (ps)	$2\Gamma(cm^{-1})$	$2\Gamma(cm^{-1})$
ν_1	991	10	41.0 ($\pm$ 1.)	0.129	0.135
ν_6	606	10	94.7 ($\pm$ 1.5)	0.056	0.056
ν_9	1174	17	33.0 ($\pm$ 1.)	0.161	0.200
ν_{10}	854	17	156.1 ($\pm$ 2.5)	0.034	0.014

A. LOW TEMPERATURE RESULTS

Our results at 10 K (Table I) coincide within experimental errors with the previously reported data,[15–17] with the only exceptionof the ν_{10} mode: the linewidth corresponding to the decay time measured for this mode in our CARS experiment is in fact about twice that reported by Trout *et al.*[17] Such a difference is difficult to explain, since for all other modes our linewidth values are slightly smaller than those of Ref. 17. In evaluating this difference, one should consider that the linewidth of ν_{10} at very low temperature is extremelly small, below the resolution of the frequency domain experiment of Ref. 17. We believe therefore that the difference between our results and those of Ref. 17 is due to the deconvolution procedure used in the frequency resolved experiment.

In analogy with what we observed for other crystals,[5–10] the values in Table I are consistent with energy decay relaxation mechanisms. According to the level scheme of Fig. 2, and considering that the lattice phonons extend only up to about 135 cm^{-1}, no three-phonon down-conversion decay channel is available for ν_6 and ν_{10}, which in fact show the longest lifetimes at low temperature. Actually, the results of experiments made at 4 K on crystals free from ^{13}C impurities[17] (see Table I) demonstrate that the linewidths of the two modes in benzene of natural isotopic composition is essentially due to the effect of isotopic impurities.

On the other hand, phonon-assisted decay to lower-lying internal levels is possible for ν_1 and ν_9, and the two modes show shorter decay times. Such a mechanism has been confirmed for ν_1 by anharmonic latice dynamics calcultions,[24] which indicated the decay into ν_{10}, with emission of a lattice phonon of about 130 cm^{-1}, as the main relaxation mechanism.

B. HIGH TEMPERATURE RESULTS

We have already mentioned that the temperature dependence of the linewidth can provide the most valuable information on the relaxation mechanism. We can summarize the expected behaviors of the different contributions to 2Γ according to the following scheme:

1. *Population decay through three-phonon processes*: The linewidth is proportional to the phonon occupation numbers, with a linear temperature dependence in the classical regime ($\hbar\omega < K_B T$).
2. *Population decay through four-phonon processes and other high-order multiphonon mechanisms*: The linewidth is proportional to products of occupation

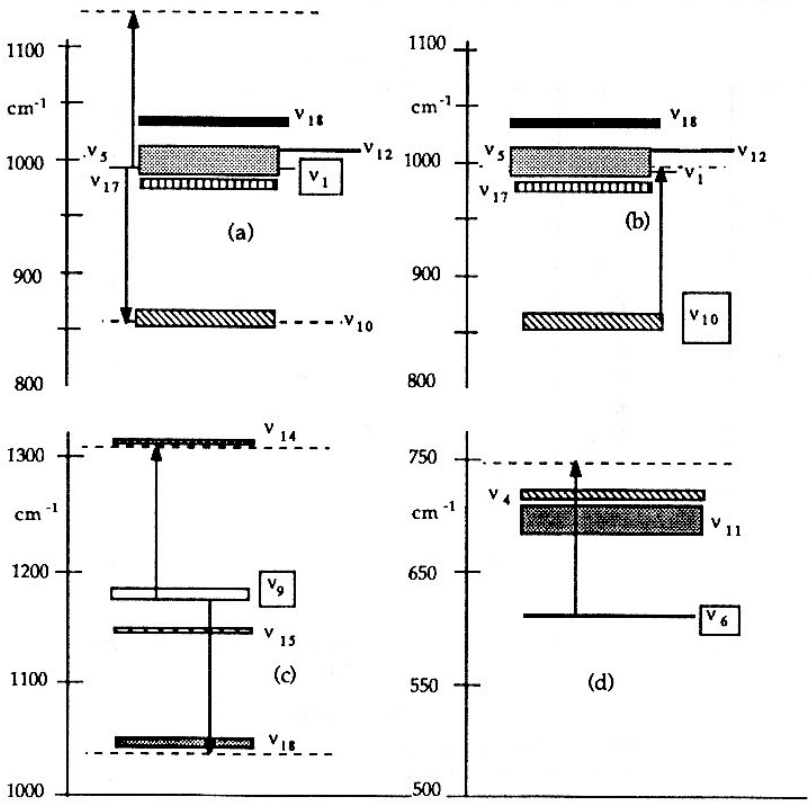

FIG. 2. Scheme of the vibrational levels of crystalline benzene. A sketch of the lattice phonon density of states is shown for each of the four studied internal modes, indicating the internal levels that can be reached in a down or up three-phonon decay process.

numbers. The resulting temperature dependence is quadratic in the temperature.

3. *Pure dephasing mechanisms due to elastic scattering of phonons*: Their effect vanishes at very low temperature, and increases with T with a nonlinear behavior.
4. *Linebroadening due to defects and impurities (including isotopic impurities)*: Although such an effect has been shown to be important at very low temperature, its temperature dependence is conceivably quite small, and in any case much less pronounced than for the other contributions.

The previous discussion provides a good basis for the interpretation of the experimental data collected in Figs. 3 to 6. The ν_1 and ν_6 modes show an undoubtedly linear temperature dependence, that can be taken as clear evidence of the dominant role of the three-phonon decay processes in the entire temperature range. With the help of the energy level scheme in Fig. 2 the possible phonons involved in the relaxation can be easily identified; for instance, ν_6 can only be coupled to ν_4 and ν_{11} by absorbing one lattice phonon with frequency between 80 and 100 cm^{-1}. The behavior of ν_9 is completely different, with a marked quadratic dependence on T. Both pure dephasing and four-phonon decay processes can be responsible for such a nonlinear contribution. Finally the situation is much less clear for ν_{10}: the weakness of this Raman band in fact made it impossible to detect the resonant CARS signal out of the nonresonant background for sample temperatures higher than 110 K. The measured temperature range is thus too small to allow us to decide unambiguously whether or not the temperature dependence of the linewidth is linear with T.

In previous papers[24,26–30] we have shown that anharmonic lattice dynamics calculations represent a fundamental support to the interpretation of the experimental data, by providing a quantitative estimate of the contributions of the different decay processes to the phonon linewidth. Calcula-

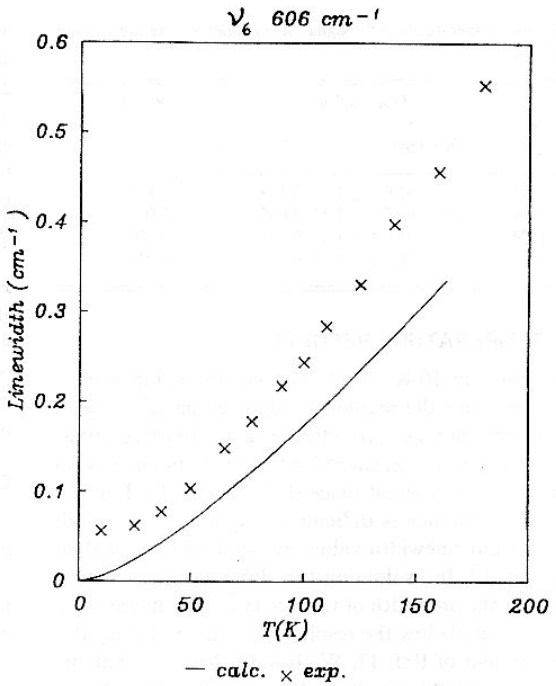

FIG. 4. Temperature dependence of the ν_6 bandwidth. crosses: experimental points; full line: calculated curve.

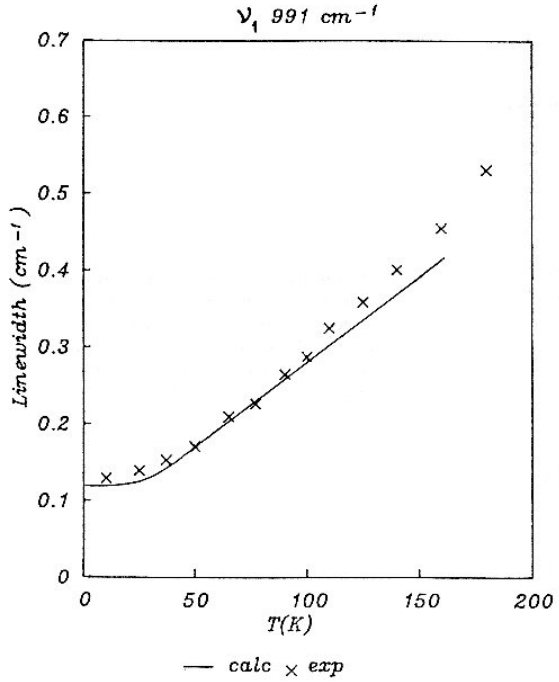

FIG. 3. Temperature dependence of the ν_1 bandwidth. crosses: experimental points; full line: calculated curve.

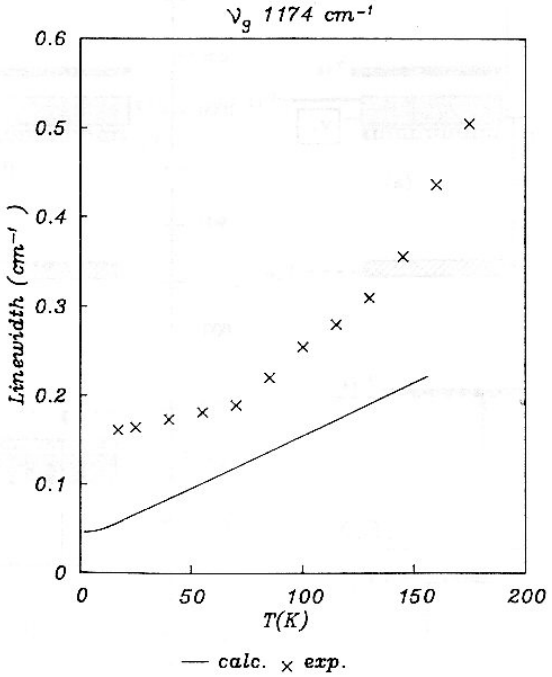

FIG. 5. Temperature dependence of the ν_9 bandwidth. crosses: experimental points; full line: calculated curve.

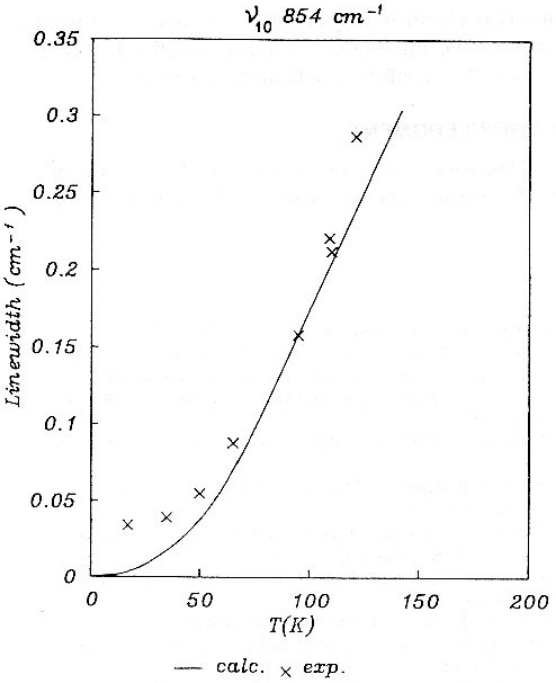

FIG. 6. Temperature dependence of the ν_{10} bandwidth. crosses: experimental points; full line: calculated curve.

tions of this kind are, however, very complex and time consuming: in the present case at least 13 internal modes (four of which are doubly degenerate) should be included (see the energy level diagram in Fig. 2) in order to account for the possible three-phonon decay pathways of ν_1, ν_6, ν_9, and ν_{10}. This is an impractical task even on a very large computer. Some approximations are then necessary if an estimate of the linewidths predicted by the anharmonic theory has to be obtained. The approximation we have adopted in the present paper is based on the following argument.

According to the theory, the phonon linewidth in a three-phonon process [see Eq. (1)] is determined by two main factors (a) the two-phonon density of states; (b) the value of the anharmonic coeficient B. While calculation of the density of states is relatively simple and fast, the evaluation of the anharmonic coefficients requires heavy computing. The expression for the cubic anharmonic coefficient coupling the phonon $\omega_i(0)$ to phonons $\omega_j(k)$ and $\omega_l(-k)$ is in fact

$$B\begin{pmatrix} i & j & l \\ 0 & k & -k \end{pmatrix} = \frac{1}{3!}\left(\frac{\hbar^3}{8\omega_i(0)\omega_j(k)\omega_l(k)}\right)^{1/2} \times \sum_{mnp}\sum_{\rho\sigma\tau} E^m_{\rho i}(0) E^n_{\sigma j}(k) \times E^p_{\tau l}(-k) D\begin{pmatrix} m & n & p \\ \rho & \sigma & \tau \end{pmatrix}, \quad (2)$$

where $E^n_{\sigma j}(k)$ is an eigenvector of the harmonic phonons and $D(^{mnp}_{\rho\sigma\tau},k)$ is an element of the third-order dynamical matrix; m, n, and p count molecules in the unit cell, and ρ, σ, and τ label the molecular coordinates (both internal and external).

In our case we are interested in processes in which one internal mode is coupled to a second internal mode and to one lattice vibration. We can then approximate expression (1) to[7]

$$B\begin{pmatrix} i & j & l \\ 0 & k & -k \end{pmatrix} = \frac{1}{3!}\left(\frac{\hbar^3}{8\omega_i(0)\omega_j(k)\omega_l(-k)}\right)^{1/2} C_{ij}(k) \quad (3)$$

where i and j label the two internal modes, l being restricted to the external vibrations. Average coefficients $C_{ij}(k)$ were obtained as

$$|C_{ij}(k)|^2 = \sum_{mnp}\sum_{\tau}\left|D\begin{pmatrix} m & n & p \\ \rho & \sigma & \tau \end{pmatrix},k\right|^2. \quad (4)$$

In Eq. (4) we have assumed that ρ and σ are the molecular normal coordinates involved in the i- and j-th crystal normal coordinates, respectively. In other words, we set in Eq. (2) $E^m_{\rho i}(0) = \delta_{i\rho}$, $E^n_{\sigma j}(k) = \delta_{j\sigma}$ and $E^p_{\tau l}(k) = \delta_{\tau l}$. This is an acceptable approximation, since the internal normal modes do not mix appreciably in the crystal. The values of the harmonic frequencies ω and of the third order force constants in $D(^{mnp}_{\rho\sigma\tau},k)$ can be obtained from a lattice dynamics calculation using intermolecular potentials available from the literature. The coefficients $C_{ij}(k)$ were calculated for different values of k and since they did not differ appreciably, an average value was taken.

The calculation of the linewidth according to expression (2) then only requires the evaluation of the two-phonon density of states and of the average B coefficient according to expressions (3) and (4). In order to avoid divergence for ω approaching zero, expression (3) was modified by introducing a damping function of the type

$$f(\omega_l) = \begin{cases} \omega_l/\omega_{tr} & \text{for } \omega_l < \omega_{tr} \\ 1 & \text{for } \omega_l > \omega_{tr} \end{cases};$$

the value of the threshold frequency ω_{tr} was set to 30 cm^{-1}, in agreement with the results of exact anharmonic calculations for N_2 crystal.[28]

In summary, the approximate calculation described here preserves the information on the average anharmonic coupling coefficients, while it fully accounts for the effect of the number of available decay channels (i.e., of the distribution of energy levels). The following decay pathways were considered:

ν_1: down conversion to ν_{17} and ν_{10}; up-conversion to ν_{12}, ν_5, and ν_{18}

ν_9: down conversion to ν_{15} and ν_{18}

ν_6: up conversion to ν_{11} and ν_4

ν_{10}: up conversion to ν_{17} and ν_1.

The average cubic coefficients and the density of states were calculated for 64 points in the reduced Brillouin zone. The intermolecular potential adopted is the same utilized for a previous calculation of the low-temperature linewidth of the ν_1 mode;[26] it consists of an atom–atom part, plus a quadrupole–quadrupole term. The molecular normal coordinates were taken from the calculation in Ref. 31.

The results of the calculations are shown in Figs. 3–6 (full lines), together with the experimental data (crosses). The agreement is generally very satisfactory, with the only exception of ν_9. The large quadratic contribution to the linewidth temperature dependence of this mode is clear evidence that relaxation mechanisms other than three-phonon scattering play a very important role: such processes are not included in our model, which is thus unable to reproduce the observed behavior for this mode.

For a correct comparison of the calculated and experimental data it is necessary to remember that the experimental points refer to crystalline benzene with natural isotopic composition whereas the curves were calculated for the pure ^{12}C species. An estimate of the effect of isotopic impurities can be made from the data of Ref. 17. These show that the low temperature width of ν_6 and ν_{10} is practically zero, in perfect agreement with our calculations. No decay channel is actually available for ν_6 and ν_{10} at very low temperature, and a vanishingly small linewidth is then calculated for these modes in the vicinity of the absolute zero. In the case of ν_1 a linewidth of 0.09 cm^{-1} was determined at 4 K for the isotopically pure crystal;[17] our calculations give a slightly larger value of 0.11 cm^{-1}.

The main relaxation mechanisms for the ν_1, ν_6, and ν_{10} modes can be found by analyzing the calculated contributions of the different decay processes to their linewidths. These are represented below in schematic form for two different temperatures.

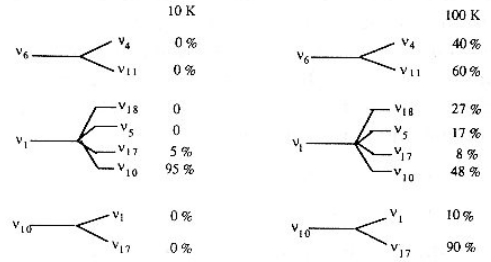

Thus, at low temperature ν_1 relaxes essentially into ν_{10}, while the increase of its linewidth with the temperature is mostly due to the anharmonic coupling with ν_{18}.

All possible decay pathways instead contribute almost evenly to the relaxation of ν_6. Finally, ν_{10} is very strongly coupled to ν_{17}, and this up-conversion process is almost entirely responsible for the temperature dependence of its bandwidth.

It is interesting to notice that all the average B coefficients coupling ν_{10} to the other modes are almost one order of magnitude larger than the other coefficients, thus showing that this mode is particularly anharmonic from the point of view of the intermolecular potential. The nature of the molecular normal coordinate, and not only the number of available decay channels, plays then a very important role in determining the anharmonic coupling, which is highly mode selective. This confirms the findings of Ref. 26.

ACKNOWLEDGMENT

This research was supported by the Italian Ministery of the "Università e Ricerca Scientifica" and by the CNR.

[1] S. Califano and V. Schettino, Int. Rev. Phys. Chem. **7**, 19 (1988).
[2] S. Califano, V. Schettino, and N. Neto, *Lattice Dynamics of Molecular Crystals*, Lectures Notes in Chemistry (Springer, Berlin, 1981).
[3] M. A. Ivanov, L. B. Kvashnina, and M. A. Krivoglaz, Sov. Phys. Sol. State **7**, 1652 (1966).
[4] C. B. Harris, R. M. Shelby, and P. A. Cornelius, Phys. Rev. Lett. **38**, 1415 (1977).
[5] L. Angeloni, R. Righini, E. Castellucci, P. Foggi, and S. Califano, J. Phys. Chem. **92**, 983 (1988).
[6] R. Righini, L. Angeloni, E. Castellucci, P. Foggi, S. Califano, and D. A. Dows, Croat. Chem. Acta **61**, 495 (1988).
[7] R. Righini, L. Angeloni, P. Foggi, E. Castellucci, and S. Califano, Chem. Phys. **131**, 463 (1989).
[8] L. Angeloni, R. Righini, Chem. Phys. Lett. **154**, 115 (1989).
[9] L. Angeloni, R. Righini, P. R. Salvi, and V. Schettino, Chem. Phys. Lett. **154**, 432 (1989).
[10] A. Tafi, P. Procacci, L. Angeloni, and R. Righini, Chem. Phys. (to be published).
[11] J. C. Bellows and P. N. Prasad, J. Chem. Phys. **70**, 1864 (1979). L. H. Hess and P. N. Prtasad, J. Chem. Phys. **72**, 573 (1980).
[12] K. Duppen, B. M. M. Hesp, and D. A. Wiersma, Chem. Phys. Lett. **79**, 399 (1981).
[13] C. L. Schosser and D. D. Dlott, J. Chem. Phys. **80**, 1394 (1984).
[14] R. Ouillon, P. Ranson, and S. Califano, Chem. Phys. **91**, 119 (1984).
[15] F. Ho, W. S. Tsay, J. Trout, and R. M. Hochstrasser, Chem. Phys. Lett. **83**, 5 (1982).
[16] S. Velsko, J. Trout, and R. M. Hochstrasser, J. Chem. Phys. **79**, 2114 (1983).
[17] J. Trout, S. Velsko, R. Bozio, P. L. Decola, and R. M. Hochstrasser, J. Chem. Phys. **81**, 4746 (1985).
[18] P. Ranson, R. Ouillon, and S. Califano, Chem. Phys. **86**, 115 (1984).
[19] P. L. Decola, R. M. Hochstrasser, and H. P. Tromsdorff, Chem. Phys. Lett. **72**, 1 (1980).
[20] B. H. Hesp and D. A. Wiersma, Chem. Phys. Lett. **75**, 423 (1980).
[21] D. D. Dlott, C. L. Schosser, and E. L. Chronister, Chem. Phys. Lett. **90**, 386 (1982).
[22] E. L. Chronister, and D. D. Dlott, J. Chem. Phys. **79**, 5286 (1983).
[23] E. L. Chronister, J. R. Hill, and D. D. Dlott, J. Chem. Phys. **82**, 159 (1985).
[24] R. Righini, Chem. Phys. **84**, 97 (1984).
[25] R. Torre, R. Righini, P. Foggi, and L. Angeloni, Appl. Phys. B (to be published).
[26] R. Righini, P. F. Fracassi, and R. G. Della Valle, Chem. Phys. Lett. **97**, 308 (1983).
[27] R. G. Della Valle, P. F. Fracassi, R. Righini, and S. Califano, Chem. Phys. **74**, 179 (1983).
[28] G. F. Signorini, P. F. Fracassi, R. Righini, and R. G. Della Valle, Chem. Phys. **100**, 315 (1985).
[29] P. Procacci, R. Righini, and S. Califano, Chem. Phys. **116**, 171 (1987).
[30] V. K. Jindal, R. Righini, and S. Califano, Phys. Rev. B **38**, 4259 (1988).
[31] G. Taddei, H. Bonadeo, M. P. Marzocchi, and S. Califano, J. Chem. Phys. **58**, 966 (1973).